Journal of Organometallic Chemistry 997 (2023) 122789

Contents lists available at ScienceDirect

Journal of Organometallic Chemistry

journal homepage: www.elsevier.com/locate/jorganchem

Gyroscope-like platinum(IV) complexes of the macrocyclic dibridgehead diphosphine $P((CH_2)_{14})_3P$ ☆,☆☆

Yun Zhu, Sourajit Dey Baksi, Nattamai Bhuvanesh, Joseph H. Reibenspies, John A. Gladysz*

Department of Chemistry, Texas A&M University, PO Box 30012, College Station, TX 77842-3012, USA

ARTICLE INFO

Article history:
Received 20 May 2023
Revised 12 June 2023
Accepted 15 June 2023
Available online 17 June 2023

Keywords:
Platinum(IV)
Dibridgehead diphosphines
Methyl complexes
Crystal structures
Gyroscopes
PtX_4 rotators

ABSTRACT

Reactions of the platinum(II) dihalide complexes *trans*-$Pt(X)_2(P((CH_2)_{14})_3P)$(X=Cl, *trans*-**4**; *Br*, *trans*-**6**) and excess X_2 give the platinum(IV) tetrahalide complexes *trans*-$Pt(X)_4(P((CH_2)_{14})_3P)$(*trans*-**5**, *trans*-**7**) in 84-95% yields. Their crystal structures are determined and the PtX*n* conformations and bond lengths compared to those of *trans*-**4** and *trans*-**6**. In one instance, a reaction of *trans*-**6** and MeMgBr (2.4 equiv) gave not the precedented product *cis*-$Pt(Me)_2(P((CH_2)_{14})_3P)$, but rather a small amount of the platinum(IV) tetramethyl complex *trans*-$Pt(Me)_4(P((CH_2)_{14})_3P)$ (*trans*-**8**), as verified crystallographically and by diagnostic NMR signals. Independent syntheses were attempted. Reactions of *trans*-**5** or *trans*-**7** with excesses of common sources of Me^- were unsuccessful. Thus, the free dibridgehead diphosphine $P((CH_2)_{14})_3P$, which can incorporate PtX_2 to give *trans*-**4** or *trans*-**6**, was treated with the $PtMe_4$ source $Pt_2Me_8(\mu\text{-}SMe_2)_2$. However, this gave instead the isomeric species *cis*-**8**, and attempts to establish *cis*/*trans* equilibria were unsuccessful.

1. Introduction

Most isolable platinum coordination complexes feature one of three oxidation states, Pt(0), Pt(II), or Pt(IV) [1]. For some time, we have been investigating the fundamental chemistry of metal complexes of *trans*-spanning dibridgehead diphosphines, such as *trans*-**II** in Scheme 1 [2–5]. These ligands generally have the formula $P((CH_2)_n)_3P$ (n = 10, 12, 14 (**1**), 16, 18) [6], although analogs with ether and *p*-phenylene containing linkages have been described [7]. Such complexes have been termed gyroscope-like [8] and rotational barriers have been studied in detail [3,4]. A number of platinum(II) [2] and more recently platinum(0) [9] adducts have been prepared. Analogous palladium(II) and nickel(II) complexes have been isolated [2a,10].

As shown in Scheme 1, complexes of the type *trans*-**II** are generally accessed from hexaolefinic precursors *trans*-**I** via three-fold intramolecular ring-closing metathesis/hydrogenation sequences. However, the free diphosphines are also capable of incorporating suitable metal fragments L_yM [6,10]. For historical reasons, there has been a particular emphasis on the chemistry of $P((CH_2)_{14})_3P$ (**1**), with fourteen methylene groups in each phosphorus-spanning tether. However, other cage sizes are now available in quantity [6b]. The isomers *cis*-**II** (Scheme 1) can sometimes be accessed from *cis*-**I** [11], and this conformational flexibility comes into play in the results below.

In developing the chemistry of a rhodium(I) adduct of **1**, *trans*-$Rh(CO)(Cl)(P((CH_2)_{14})_3P)$, (*trans*-**2**), we discovered an oxidative addition process that afforded the octahedral rhodium(III) complex *trans*-**3** (Scheme 1, bottom) [3]. Close relatives of *trans*-**2** could be used as catalyst precursors for olefin hydroformylation [3a], for which rhodium(III) intermediates would be assumed [12]. Given the role of platinum(IV) species in catalytic carbon-hydrogen bond activation processes [13], we have sought to access platinum adducts of **1** in higher oxidation states. Accordingly, in this paper we describe our initial syntheses and characterization of platinum(IV) species of the types *trans*- and *cis*-**II**.

2. Results

First, a CH_2Cl_2 solution of the light yellow platinum(II) dichloride complex *trans*-$Pt(Cl)_2(P((CH_2)_{14})_3P)$ (*trans*-**4**, Scheme 2) was treated with chlorine that was generated *in situ* from aqueous NaOCl and HCl [14]. A $^{31}P\{^1H\}$ NMR spectrum showed complete conversion to a new species over the course of 0.5 h, and workup gave the target platinum(IV) tetrachloride complex *trans*-$Pt(Cl)_4(P((CH_2)_{14})_3P)$ (*trans*-**5**) as a yellow solid in 95% yield. This material, as most new complexes below, was characterized by NMR

☆ submitted to *J. Organomet. Chem.* for the special issue on nanoscale organometallics.

☆☆ All titles are given in the capitalization format of the original article.

* Corresponding author.
E-mail address: gladysz@chem.tamu.edu (J.A. Gladysz).

https://doi.org/10.1016/j.jorganchem.2023.122789
0022-328X/

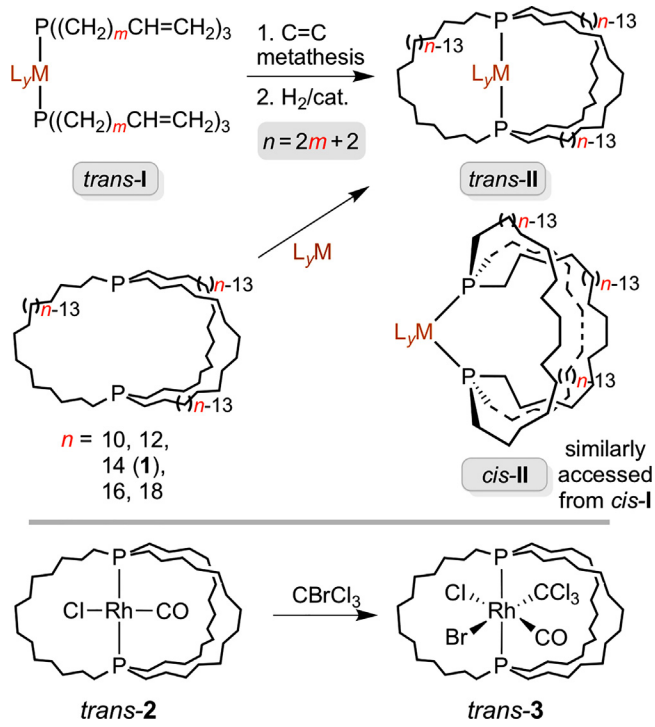

Scheme 1. Synthetic approaches to gyroscope-like complexes *trans*-**II** (top), and conversion of a rhodium(I) adduct to a rhodium(III) adduct (bottom).

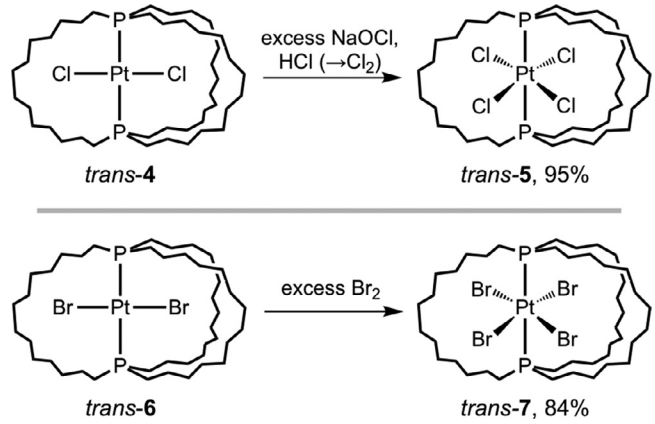

Scheme 2. Syntheses of platinum(IV) tetrahalide complexes.

spectroscopy (^{1}H, ^{13}C{^{1}H}, ^{31}P{^{1}H}) and microanalysis, as summarized in the experimental section.

Next, a diethyl ether solution of the analogous platinum(II) dibromide complex *trans*-**6** was treated with Br_2 (ca. 12 equiv). As shown in Scheme 2, workup gave the target platinum(IV) tetrabromide complex *trans*-**7** as a red-orange solid in 84% yield. Alternatively, *trans*-**7** was equally well prepared by the reaction of the dichloride complex *trans*-**4** and excess Br_2. Importantly, *trans*-**5** and *trans*-**7** lack P-PtX_4-P conformations in which all three $P(CH_2)_{14}P$ linkages become symmetry equivalent. Nonetheless, only seven CH_2 ^{13}C{^{1}H} NMR signals were observed at room temperature, indicating rapid PtX_4 rotation on the NMR time scale. When ^{13}C{^{1}H} NMR spectra of *trans*-**7** were recorded in CD_2Cl_2 at −50 °C, no decoalescence phenomena were apparent. However, upon further cooling, precipitation commenced.

As seen for other complexes of the type *trans*-**II**, three of the ^{13}C{^{1}H} signals of *trans*-**5** and *trans*-**7** were virtual triplets [15]. Assignments were made by 2D NMR experiments depicted in Fig. 1. First, a ^{1}H,^{1}H COSY spectrum allowed assignment of the PCH_2, PCH_2CH_2, and $PCH_2CH_2CH_2$ signals. Second, ^{1}H,^{13}C{^{1}H} HSQC and ^{1}H,^{13}C{^{1}H} gHMBC spectra identified the respective CH_2 signals. The PCH_2 signals of *trans*-**5** and *trans*-**7** exhibited the highest J_{CP} values (15.6–16.4 Hz, δ 19.7–23.7 ppm), followed by the $PCH_2CH_2CH_2$ (6.9–7.1 Hz, δ 28.8–29.7 ppm) and PCH_2CH_2 signals (1.9–1.9 Hz, δ 21.6–22.3 ppm). The corresponding resonances of the platinum(II) precursors *trans*-**4** and *trans*-**6** exhibit similar coupling constant and chemical shift trends ($CDCl_3$: 16.3–16.7 Hz, δ 21.3–22.7 ppm; 6.8–6.8 Hz, δ 30.0–29.9 ppm; <2 Hz, δ 23.1–23.2 ppm) [12a].

The stereochemistry assigned to *trans*-**5** and *trans*-**7** is not rigorously demanded by the ^{13}C{^{1}H} NMR data. Complexes of the type *cis*-**II** (Scheme 1) exhibit similar virtual coupling patterns, and the $P(CH_2)_nP$ linkages can often exchange by "jump rope" mechanisms [2d,11]. However, ^{31}P{^{1}H} NMR spectra are available for both *trans* and *cis* isomers of a number of closely related complexes $Pt(X)_4(PR_3)_2$ [16]. For X/R = Cl/Me, Cl/*n*-Bu, and Br/Me, the J_{PPt} values are 1550–1462 Hz for the *trans* isomers, and 2081–2015 Hz for *cis*. Those of *trans*-**5** and *trans*-**7** (1552–1480 Hz) are unambiguously in the *trans* range.

To further substantiate these assignments, *trans*-**5** and *trans*-**7** were crystallized and the X-ray structures determined as outlined in Table 1 and the experimental section. In the case of *trans*-**7**, two independently grown crystals were examined and data for both are included. In the case of *trans*-**5**, each $(CH_2)_{14}$ segment was disordered over two positions in a chiral space group. Thermal ellipsoid plots are provided in Fig. 2, and key metrical parameters are presented in Table 2, together with those of the platinum(II) analogs. Additional analyses are given below.

In a reaction originally designed to give the dimethyl complex $Pt(Me)_2(P((CH_2)_{14})_3P)$ (**9**), the dibromide complex *trans*-**6** was treated with MeMgBr (2.4 equiv) in diethyl ether (Scheme 3, top). In an aerobic workup, a MeOH quench was followed by chromatography on Florisil. Workup of one fraction gave a white crystalline solid. The X-ray structure, depicted in Fig. 2, surprisingly revealed two independent molecules of the platinum(IV) tetramethyl complex *trans*-$Pt(Me)_4(P((CH_2)_{14})_3P)$ (*trans*-**8**). The data suggested some disorder in the $(CH_2)_{14}$ segments, but none in the $PtMe_4$ rotator. The $PtCH_3$ ^{1}H NMR signal was a triplet due to phosphorus coupling (δ −0.19 ppm, J_{HP} = 5.1 Hz) and exhibited the expected platinum satellites (J_{HPt} = 43.8 Hz). A *cis* isomer should give, in the absence of unusual dynamic phenomena, two $PtCH_3$ ^{1}H NMR signals.

Unfortunately, this synthesis could not be repeated, blocking deeper probes of the NMR and other properties. Additional context is provided by the reaction of the dichloride complex *trans*-**4** and MeLi [2d]. As shown in Scheme 3 (middle), this affords the crystallographically characterized *cis* platinum(II) dimethyl complex *cis*-$Pt(Me)_2(P((CH_2)_{14})_3P)$ (*cis*-**9**) in 77% yield. The *trans* → *cis* isomerization, which is interpreted below in the framework of the *trans* effect, renders the one-off isolation of *trans*-**8** even more mysterious.

Alternative routes to *trans*-**8** or the isomer *cis*-**8** were considered. First, the platinum(IV) tetrahalide complexes *trans*-**5** and *trans*-**7** were combined with reagents such as MeLi, MeMgBr, and $ZnMe_2$ (≥4.2 equiv). In all cases, NMR analyses showed reductions to known platinum(II) complexes (*cis*-**9** or *trans* Pt(Me)(X) species [2d]). A second approach was motivated by the reactions of $P((CH_2)_{14})_3P$ (**1**) and L_yM sources in Scheme 1 (e.g., $PtCl_2$), which give the gyroscope-like complexes *trans*-**II** [2a,10]. What would happen with platinum(IV) sources?

The diplatinum octamethyl complex $Pt_2Me_8(\mu\text{-}SMe_2)_2$ readily serves as a $Pt(Me)_4$ equivalent, although reactions with the monophosphines PMe_2Ph and $PMePh_2$ give the *cis* adducts *cis*-$Pt(Me)_4(PMe_zPh_{3-z})_2$ [17]. As shown in Scheme 3 (bottom), a reaction with **1** analogously gave *cis*-**8**. The stereochemistry was

Table 1
Summary of crystallographic data.

	trans-**5**	*trans*-**7**[a]	*trans*-**8**
empirical formula	$C_{42}H_{84}Cl_4P_2Pt$	$C_{42}H_{84}Br_4P_2Pt$	$C_{46}H_{96}P_2Pt$
formula weight	987.92	1165.76	906.25
temperature [K]	110.0	110.0	110.0
diffractometer	Kappa	Venture/APEXII	Venture
wavelength [Å]	1.54178	1.54178/0.70173	1.54178
crystal system	tetragonal	monoclinic	triclinic
space group	P 4_3	P 1 2_1/c 1	P-1
unit cell dimensions:			
a [Å]	16.3335(4)	16.7199(11)/16.6211(10)	13.8129(10)
b [Å]	16.3335(4)	19.0816(12)/19.0349(11)	14.5821(11)
c [Å]	17.6999(8)	15.2974(10)/15.2894(9)	26.278(2)
α [°]	90	90	104.892(2)
β [°]	90	103.358(2)/103.263(3)	93.778(3)
γ [°]	90	90	109.828(3)
V [$Å^3$]	4722.0(3)	4748.5(5)/4708.0(5)	4743.2(6)
Z	4	4	4
ρ_{calc} [Mg/m^{-3}]	1.390	1.631/1.645	1.269
μ [mm^{-1}]	8.467	10.293/6.470	6.355
F(000)	2048	2336	1920
crystal size [mm^3]	0.4 × 0.3 × 0.3	0.085/0.7 × 0.054/0.5 × 0.047/0.3	0.15 × 0.13 × 0.017
Θ limit [°]	2.705 to 79.028	2.716 to 70.302/3.904 to 55.198	3.310 to 60.495
index range (*h, k, l*)	−20, 20; −20, 20; −19, 22	−20, 20/−21, 21; −23, 23/−24, 24; −18, 18/−19, 19	−15, 15; −15, 16; −29, 29
reflections collected	54,027	57,811/174,120	86,542
independent reflections	9454	9030/10,859	14,213
R(int)	0.0671	0.0456/0.1417	0.0585
completeness to Θ	99.8	99.9/99.5	99.2
max. and min. transmission	1.0 and 0.35	0.2751/0.372 and 0.1468/0.052	0.4649 and 0.2424
data, restraints, parameters	9454/805/824	9030/10,859, 0/0, 442/443	14,213, 1571, 891
goodness-of-fit on F^2	1.042	1.087/1.067	1.037
R indices (final) [$I > 2\sigma(I)$]			
R_1	0.0793	0.0280/0.0370	0.0974
wR_1	0.2036	0.0713/0.0842	0.2462
R indices (all data)			
R_2	0.1088	0.0332/0.0584	0.1064
wR_2	0.2365	0.0796/0.0975	0.2560
largest diff. peak and hole [$eÅ^{-3}$]	0.926/−1.021	1.317/1.96 and −1.104 /−2.42	3.197 and −3.213

[a]Two independent structure determinations (data separated by slashes).

Table 2
Key crystallographic distances [Å] and angles [°].

	trans-**4** ($PtCl_2$)	*trans*-**5** ($PtCl_4$)	*trans*-**6** ($PtBr_2$)	*trans*-**7** (1)[a] ($PtBr_4$)	*trans*-**7** (2)[a] ($PtBr_4$)	*trans*-**8** (1)[b] ($PtMe_4$)	*trans*-**8** (2)[b] ($PtMe_4$)	*cis*-**9** ($PtMe_2$)
P···P	4.611	4.748	4.625	4.814	4.808	4.615	4.641	3.602
Pt-P	2.3051(8)	2.376(3)	2.3100(13)	2.4097(10)	2.4024(12)	2.309(3)	2.324(3)	2.2844(11)
	2.3082(8)	2.372(3)	2.3169(13)	2.4055(10)	2.4071(12)	2.308(3)	2.319(3)	2.2818(11)
Pt-Cl	2.3165(10)	2.322(4)	2.4281(8)	2.4751(4)	2.4681(5)	2.154(12)	2.167(13)	2.105(4)
or	2.3082(8)	2.324(4)	2.4313(8)	2.4707(5)	2.4860(5)	2.137(14)	2.146(13)	2.106(5)
Pt-Br		2.263(6)		2.4799(4)	2.4635(5)	2.146(15)	2.120(14)	
or		2.284(8)		2.4974(4)	2.4590(6)	2.145(16)	2.171(14)	
Pt-C								
P-Pt-P	176.75(3)	177.90(15)	177.10(5)	177.44(3)	177.29(4)	176.46(12)	176.52(11)	104.15(4)
P-Pt-Cl	85.98(3)	92.87(14)	86.10(3)	89.76(2)	89.62(3)	88.1(4)	89.0(4)	86.76(16)
or	93.10(3)	89.04(17)	93.28(3)	90.32(3)	90.72(3)	88.5(4)	89.2(3)	167.83(17)
P-Pt-Br	88.88(3)	88.93(13)	88.46(3)	91.68(2)	91.86(3)	88.3(5)	92.3(4)	87.06(17)
or	92.11(3)	90.15(15)	92.27(3)	88.88(3)	88.75(3)	91.2(5)	89.2(4)	167.78(17)
P-Pt-C				90.52(3)	90.60(3)	89.8(5)	89.9(4)	
				92.23(3)	91.98(3)	90.9(5)	87.6(3)	
				88.19(3)	88.07(3)	94.0(5)	91.0(4)	
				88.58(2)	88.55(3)	89.4(5)	92.1(4)	
Cl-Pt-Cl	178.10(3)	91.15(17)	173.508(18)	91.436(15)	91.241(19)	94.1(6)	91.8(5)	82.6(2)
or		93.40(2)		89.227(16)	89.338(19)	83.8(8)	90.4(6)	
Br-Pt-Br		92.20(3)		87.408(16)	87.71(2)	88.6(6)	91.5(7)	
or		83.30(3)		91.948(15)	91.722(18)	93.5(8)	86.4(7)	
C-Pt-C		175.50(2)		176.348(15)	176.72(2)	177.0(7)	177.1(6)	
		176.70(3)		178.954(15)	179.21(2)	176.6(6)	176.4(6)	
approx. cage radius[c]	6.48	6.54	6.53	6.36	6.34	6.60	6.64	–

[a]Values for two independent structure determinations. [b]Values for the two independent molecules in the unit cell. [c]Average distance of the four innermost carbon atoms of all three $P(CH_2)_{14}P$ chains from the P···P vector.

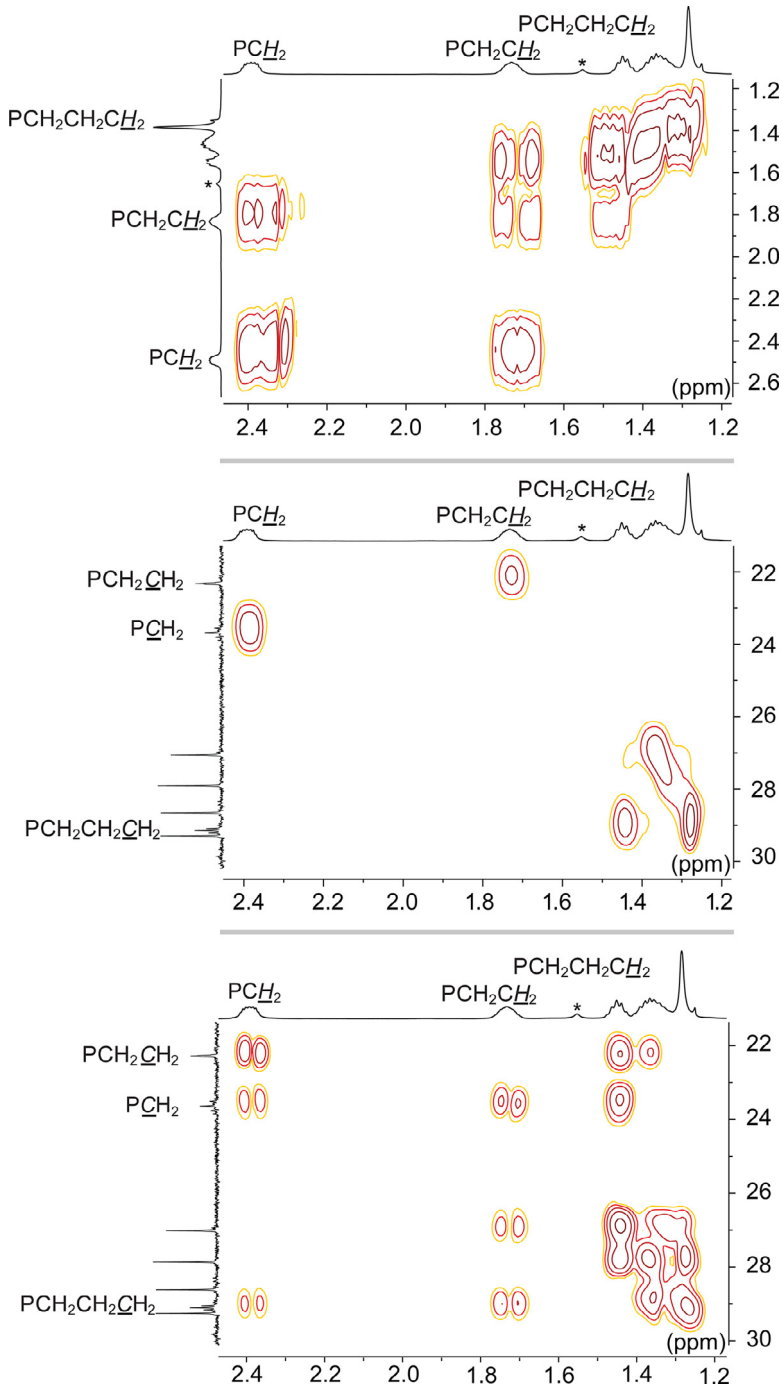

Fig. 1. $^{1}H,^{1}H$ gCOSY (top) $^{1}H,^{13}C\{^{1}H\}$ HSQC (middle), $^{1}H,^{13}C\{^{1}H\}$ gHMBC (bottom) spectra of *trans*-**7** (500 MHz, $CDCl_3$).The * indicates a solvent-based impurity.

evidenced by two $PtCH_3$ ^{1}H and ^{13}C NMR signals, one for the groups *trans* to the phosphorus atoms, and another for those *trans* to each other. The J_{PPt} value was much lower than that of *trans*-**8** (1215 vs. 2033 Hz). Importantly, these values are closely mirrored by those of *cis*- and *trans*-$Pt(Me)_4(PMe_3)_2$ (1292 vs. 2120 Hz) [18,19]. Only one set of $P(CH_2)_{14}P$ $^{13}C\{^{1}H\}$ NMR resonances was observed at ambient temperature.

Curiously, analogous reactions with various platinum tetrahalide sources (e.g., $PtCl_4$, K_2PtCl_6, *trans*-$PtBr_4(SMe_2)_2$ [20]) were not successful. In some cases, ^{31}P NMR evidence for the dichloride *trans*-**4** or the diphosphine dioxide of **1** was obtained. Sometimes *cis*-**II** and *trans*-**II** can be thermally equilibrated [2d,11]. However, when a toluene solution of *cis*-**8** was heated to 80 °C, $^{31}P\{^{1}H\}$ NMR indicated complete decomposition over the course of 2 h. Given the inability to reproduce the synthesis of *trans*-**8**, the reverse reaction could not be studied [21].

3. Discussion

The routes to the platinum(IV) tetrahalide complexes *trans*-**5** and *trans*-**7** in Scheme 2 have abundant precedent. For example, the reaction of the dichloride complex *trans*-$Pt(Cl)_2(PEt_3)_2$ and Cl_2 gives the tetrachloride *trans*-$Pt(Cl)_4(PEt_3)_2$ (86%) [22]. Similarly, the dibromide complex *trans*-$Pt(Br)_2(PEt_3)_2$ and Br_2 afford *trans*-$Pt(Br)_4(PEt_3)_2$ (85%) [23], which exhibits a J_{PPt} value close to that of *trans*-**7** (1495–1452 vs. 1480 Hz). Literature precedent for the syn-

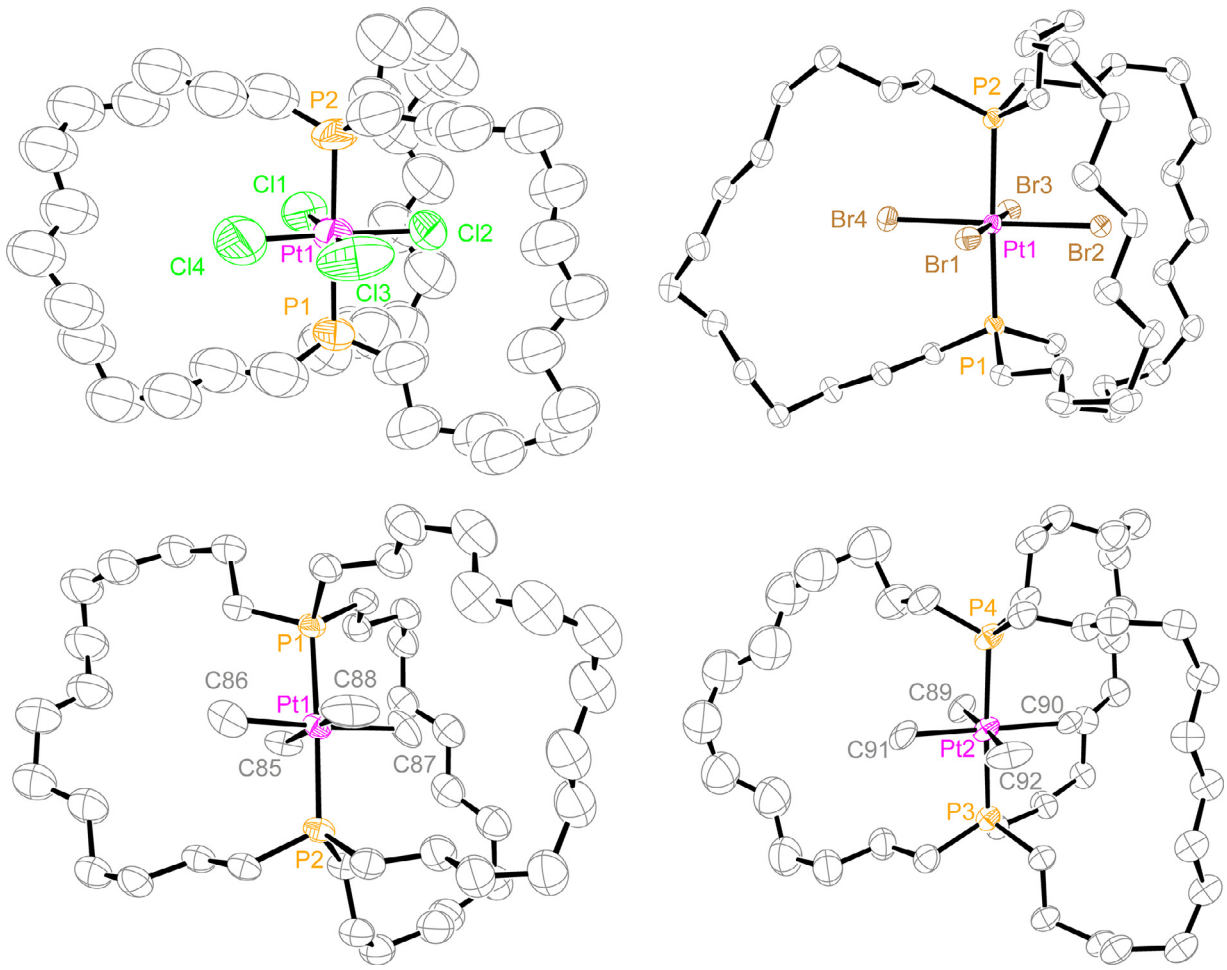

Fig. 2. Thermal ellipsoid plots (50% probability level) for *trans*-**5** (upper left; dominant $(CH_2)_{14}$ conformations only), *trans*-**7** (upper right) and *trans*-**8** (bottom; two independent molecules in unit cell).

thesis of *cis*-**8** (Scheme 3) was noted above [17], but the means by which *trans*-**8** forms remains a puzzle, especially in view of electronic considerations below [21]. For *trans*-**5** and *trans*-**7**, metathesis/hydrogenation sequences analogous to those in Scheme 1 (top) – i.e., from precursors of the type *trans*-$Pt(X)_4(P((CH_2)_6CH{=}CH_2)_3)_2$ – could also have been investigated. Such routes have allowed access to a number of octahedral rhenium and osmium complexes [5]. However, alternative macrocyclization modes are often observed (e.g., *intra*ligand ring closing metathesis), and yields vary.

The relative sizes of the thermal ellipsoids in Fig. 2 and esd values in Table 2 provide a rough measure of the quality of each crystal structure. Despite the complicating disorder in the tetrachloride complex *trans*-**5**, the bond lengths and angles about platinum are accurately determined. The former are quite close to those of *trans*-$Pt(Cl)_4(PEt_3)_2$ (Pt-Cl, 2.263(6)–2.324(4) vs. 2.332(5) Å; Pt-P, 2.372(3)–2.376(3) vs. 2.393(5) Å) [24]. For the tetrabromide *trans*-**7**, the metrical parameters are in good agreement with those of *trans*-$Pt(Br)_4(PEt_3)_2$ (Pt-Br, 2.4590(6)–2.4974(4) vs. 2.4713(3)–2.4753(3) Å; Pt-P, 2.4024(12)–2.4097(10) vs. 2.4089(7) Å [23]. In both series, the platinum-halide and platinum-phosphorus bonds in the dihalides are somewhat shorter than those in the tetrahalides (Table 2). This also holds for the methyl complexes *cis*-**9** and *trans*-**8**, and the P···P distances in the halide complexes.

The dibromide *trans*-**6** and tetrabromide *trans*-**7** represent the first time we have had high quality crystal structures of square planar and octahedral gyroscope-like complexes with the same ligand sets. Fig. 3 compares views down the P-Pt-P bond axes. In both *trans*-**4** and *trans*-**6**, the X-Pt-X linkages are coincident with one of those in *trans*-**5** and *trans*-**7**. In other words, the immediate coordination sphere is not greatly affected by the introduction of a second *trans* X-Pt-X moiety. The overall macrocycle conformations are also quite similar in the two platinum(II) and two platinum(IV) species. The corresponding views of the two independent molecules of the tetramethyl complex *trans*-**8** are given for comparison (Fig. 3, bottom).

We sought to probe whether the two additional equatorial ligands in the tetrahalide complexes affected the overall radii of the diphosphine cages. Thus, the average distances of the four innermost $(CH_2)_{14}$ carbon atoms from the P-P vectors (twelve values) were calculated. As summarized in Table 2, no trends were apparent. In this context, the radii of the MX_n rotators can be calculated by taking the (longest) metal-halide bond and adding the van der Waals radius of the halide (Cl, 1.75 Å; Br, 1.85 Å) [25]. Thus, the radii of the PtX_2 and PtX_4 rotators are nearly identical (X = Cl, 4.06 Å [2a] and 4.18 Å; *X* = Br, 4.28 Å [2a] and 4.32 Å). These values are somewhat less than those of the cage radii (Table 2) *minus* the van der Waals radius of carbon (1.70 Å), supportive of ample clearance for rapid rotation.

With respect to their geometric isomers, the numbers of *trans* methyl groups are minimized in *cis*-**8** and *cis*-**9** (Scheme 3). Methyl ligands are strong σ donors [26], much more so than halide lig-

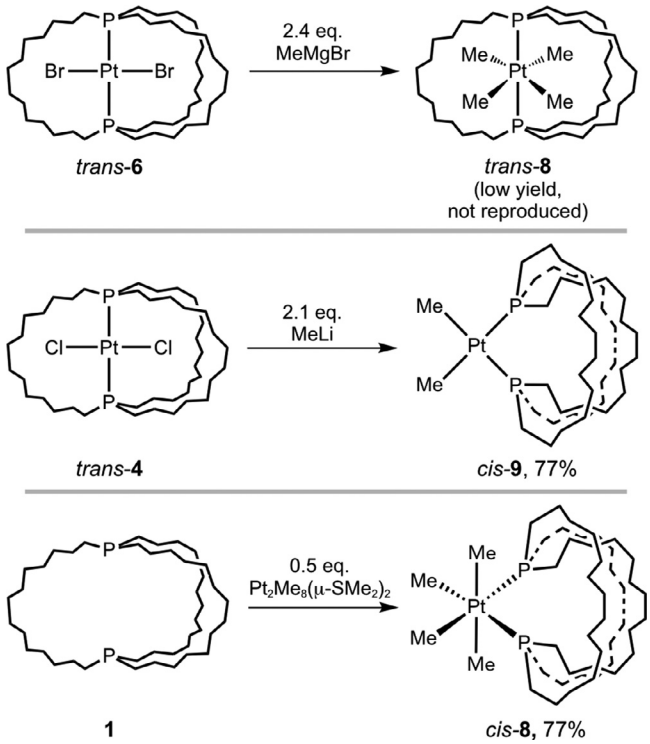

Scheme 3. Syntheses of platinum(IV) tetramethyl and platinum(II) dimethyl complexes.

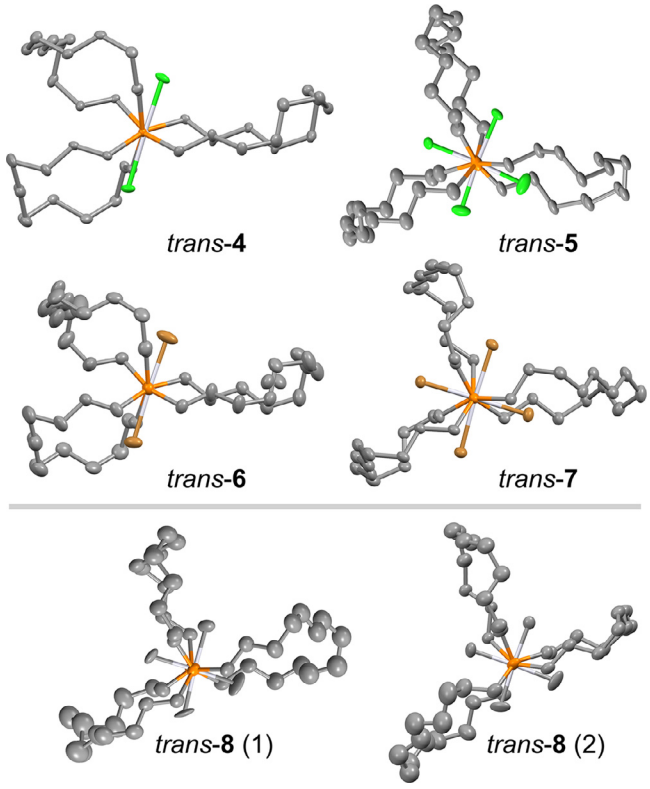

Fig. 3. Top and middle: comparison of the conformations of PtX_2 and PtX_4 rotators in the crystalline chloride and bromide complexes. Bottom: the conformations of the $PtMe_4$ rotators in the two independent molecules in crystalline *trans*-**8**.

ands. Within the rubric of the *trans* influence [27,28], it intuitively follows that methyl ligands would avoid *trans* relationships when alternatives are accessible. We have computationally investigated *cis*/*trans* equilibria for a related series of complexes $Pt(X)(Y)(PEt_3)_2$ (X/Y = Ph/Ph, Et/Et, Me/Me, Ph/Cl, Et/Cl, Me/Cl, Cl/Cl) [2d]. Under all conditions examined (gas phase and polar and nonpolar solvents), the Me/Me and Et/Et adducts gave the highest proportion of *cis* isomers. Largely parallel trends were found for the corresponding adducts of **1**, $Pt(X)(Y)((P((CH_2)_{14})_3P)$ [2d].

All the dibridgehead diphosphines in Scheme 1 are capable of *in*/*out* isomerism, and these equilibria are detailed elsewhere [6]. Regarding Schemes 2 and 3, note that the *trans* complexes feature *in,in*-**1**, and the *cis* complexes a "bent" *out,out*-**1**. However, pyramidal inversion at phosphorus – a process normally requiring >30 kcal/mol [29] – is not required, as these macrocycles are topologically capable of turning themselves inside out [6], resulting in an apparent double inversion and circumventing the higher energy pathway.

Although no rate constants or activation parameters are available, the NMR data for *trans*-**5** and *trans*-**7** suggest surprisingly low barriers to PtX_4 rotation. A number of octahedral derivatives of the dibridgehead diphosphine **1** have been reported. Those with $Os(X)_2(CO)_2$ and $Re(X)(CO)_3$ (X = Cl, Br) rotators also exhibit quite low barriers, a phenomenon that has been analyzed in detail [5,8]. Ground state strain, which can be intuited in Fig. 3 (~eclipsed Pt-X/macrocycle units), is likely one factor. However, the rhodium complex *trans*-**3** (Scheme 1) [3b] exhibits a higher barrier due to the steric bulk of the CCl_3 ligand, resulting in three sets of $P(CH_2)_{14}P$ $^{13}C\{^1H\}$ NMR signals at room temperature. Substituting any of the halide ligands in *trans*-**5** or *trans*-**7** with a phenyl ligand should also, by analogy to trends seen in square planar complexes of **1** [2b,3d] and the $Re(X)(CO)_3$ systems [5], slow rotation on the NMR time scale.

In summary, this work affords a practical entry into unusual platinum(IV) complexes with sterically protected $PtCl_4$ and $PtBr_4$ rotators, and related *cis* tetramethyl species capable of additional types of dynamic behavior. Apropos to this special issue on nanoscale organometallics, one aspect targeted for future development is the synthesis of analogs with dipolar rotators, as exemplified by the rhodium complexes *trans*-**2** and *trans*-**3** (Scheme 1). Dipolar species can be manipulated by electric fields. They can in theory be oriented by static electric fields (molecular compasses) or driven unidirectionally by rotating electric fields (molecular gyroscopes) [8,30].

4. Experimental section

General. Reactions were conducted under inert atmospheres unless noted, and workups were carried out in air. Chemicals were treated as follows: CH_2Cl_2, diethyl ether, toluene and THF, dried and degassed using a Glass Contour solvent purification system; hexanes (98.5% Sigma-Aldrich), NaOCl (2.5% w/w, Ricca Chemical), HCl (36.5–38%, VWR), Br_2 (99.5%, Sigma-Aldrich), MeMgBr (3.0 M in diethyl ether, Alfa Aesar), K_2PtCl_6 (98%, Ambeed), $PtCl_4$ (99%, Pressure Chemical), $CDCl_3$, CD_2Cl_2 (2 × Cambridge Isotope Laboratories), celite (EMD), $MgSO_4$ (Fisher Chemical), $NaHCO_3$ (99.7%, VWR), Florisil® (Fluka Analytical), used as received.

All instrumentation and characterization protocols were identical to those in a previous full paper in this series [2d]. NMR spectra were referenced as follows (δ/ppm): ^1H, residual $CHCl_3$ (7.26) or $CDHCl_2$ (5.32); ^{13}C NMR, $CDCl_3$ (77.16) or CD_2Cl_2 (53.5); ^{31}P NMR, external H_3PO_4 (0.00).

***trans*-Pt(Cl)$_4$(P((CH$_2$)$_{14}$)$_3$P) (*trans*-5)**. Under air, a round bottom flask was charged with *trans*-$Pt(Cl)_2(P((CH_2)_{14})_3P)$ (*trans*-**4**; 0.0395 g, 0.0431 mmol) [2a], CH_2Cl_2 (4.0 mL), and NaOCl (7.0 mL,

ca. 2.5% w/w in water). Concentrated HCl (1.0 mL, 12 N) was slowly added with stirring to generate Cl_2 [14]. After the reaction was complete by $^{31}P\{^1H\}$ NMR (0.5 h), saturated aqueous $NaHCO_3$ was slowly added until gas evolution ceased. The organic phase was separated, and the aqueous phase extracted with CH_2Cl_2 (5.0 mL × 3). The combined organic phases were dried ($MgSO_4$) and the solvent removed by rotary evaporation to give *trans*-**5** (0.0389 g, 0.0394 mmol, 91%) as a yellow solid, mp 97–104 °C. Calcd. for $C_{42}H_{84}Cl_4P_2Pt$ (987.95): C 51.06; H 8.57. Found: C 51.17; H 8.59.

NMR ($CDCl_3$, δ/ppm): ^1H (500 MHz) 2.16–2.08 (m, 12H, PCH_2), 1.74–1.64 (m, 12H, PCH_2CH_2), 1.46–1.39 (m, 12H, $PCH_2CH_2CH_2$), 1.39–1.24 (m, 48H, remaining CH_2); $^{13}C\{^1H\}$ (126 MHz) 29.7 (virtual t [15], J_{CP} = 6.9 Hz, $PCH_2CH_2CH_2$), 28.8 (s, CH_2), 28.6 (s, CH_2), 27.7 (s, CH_2), 26.9 (s, CH_2), 21.6 (virtual t [15], J_{CP} = 1.9 Hz, PCH_2CH_2), 19.7 (virtual t [15], J_{CP} = 15.6 Hz, PCH_2); $^{31}P\{^1H\}$ (202 MHz) 1.0 (s, J_{PPt} = 1552 Hz) [31].

***trans*-Pt(Br)$_4$(P((CH$_2$)$_{14}$)$_3$P) (*trans*-7).** Under air, a round bottom flask was charged with *trans*-Pt(Br)$_2$(P((CH$_2$)$_{14}$)$_3$P) (*trans*-**6**; 0.3677 g, 0.3655 mmol) [2a] and diethyl ether (6.5 mL), and Br_2 (0.25 mL, 4.85 mmol) was added with stirring. After 18 h, the solvent and excess Br_2 were removed by oil pump vacuum. The residue was washed with diethyl ether (10 mL) to give *trans*-**7** (0.3595 g, 0.3084 mmol, 84%) as a red/orange solid that started to blacken at 190 °C and melted at 211 °C. Calcd. for $C_{42}H_{84}Br_4P_2Pt$ (1165.75): C 43.27; H 7.26. Found: C 42.98; H 7.24.

NMR ($CDCl_3$, δ/ppm): ^1H (500 MHz) 2.46–2.28 (m, 12H, PCH_2), 1.82–1.66 (m, 12H, PCH_2CH_2), 1.48–1.42 (m, 12H, $PCH_2CH_2CH_2$), 1.42–1.19 (m, 48H, remaining CH_2); $^{13}C\{^1H\}$ (126 MHz) 29.3 (s, CH_2), 29.1 (virtual t [15], J_{CP} = 7.1 Hz, $PCH_2CH_2CH_2$), 28.7 (s, CH_2), 27.9 (s, CH_2), 27.1 (s, CH_2), 23.7 (virtual t [15], J_{CP} = 16.4 Hz, PCH_2), 22.3 (virtual t [15], J_{CP} = 1.9 Hz, PCH_2CH_2); ^{31}P (202 MHz) −13.6 (s, J_{PPt} = 1480 Hz) [31]. MS (APCI, *m/z*): 1184.2694 ([$M + H + H_3O$]$^+$, 2%), 1085.3186 ([M-Br]$^+$, 39%), 1005.3938 ([M-2Br]$^+$, 43%), 925.4844 ([M-3Br]$^+$, 29%), 844.5598 ([M-4Br]$^+$, 5%).

***trans*-Pt(Me)$_4$(P((CH$_2$)$_{14}$)$_3$P) (*trans*-8).** A Schlenk flask was charged with *trans*-**6** (0.1248 g, 0.1241 mmol) [2a] and diethyl ether (12.0 mL) and cooled to 0 °C. Then MeMgBr (3.0 M in ethyl ether; 0.10 mL, 0.30 mmol) was added with stirring. The cold bath was removed. After 40 h, a $^{31}P\{^1H\}$ NMR spectrum showed substantial conversion to product. A few drops of MeOH were added and the sample exposed to air. After 1 h, the mixture was filtered through celite, which was washed with diethyl ether. The solvent was removed from the filtrate and washings by rotary evaporation. The residue was chromatographed on florisil (1:8 v/v hexanes/CH_2Cl_2). The solvent was removed by rotary evaporation to give *trans*-**8** as a white solid. See the text for remarks on the reproducibility of this experiment.

NMR ($CDCl_3$, δ/ppm): ^1H (500 MHz) 1.90–1.77 (m, 12H, PCH_2), 1.50–1.41 (m, 12H, PCH_2CH_2), 1.41–1.18 (m, 60H, remaining CH_2), −0.19 (t, 12H, J_{HP} = 5.1 Hz, J_{HPt} = 43.8 Hz [31], $PtCH_3$); $^{13}C\{^1H\}$(126 MHz) 29.7 (s [32], $PCH_2CH_2CH_2$), 29.0 (s, CH_2), 28.7 (s, CH_2), 27.8 (s, CH_2), 27.2 (s, CH_2), 22.1 (s, PCH_2CH_2), 21.2 (s [32], PCH_2), −18.1 (s [32], $PtCH_3$); $^{31}P\{^1H\}$ (202 MHz) −27.4 (s, J_{PPt} = 2033 Hz) [31].

***cis*-Pt(Me)$_4$(P((CH$_2$)$_{14}$)$_3$P) (*cis*-8).** A Schlenk flask was charged with $Pt_2Me_8(\mu\text{-}SMe_2)_2$ (0.0563 g, 0.0887 mmol) [17], (*in,in/out,out*)-P((CH$_2$)$_{14}$)$_3$P (**1**; 0.1126 g, 0.1729 mmol) [6], and CH_2Cl_2 (5 mL) with stirring. After 15 min, a $^{31}P\{^1H\}$ NMR spectrum indicated >99% conversion to product. The solvent was removed by rotary evaporation and diethyl ether was added. The solid was isolated by filtration, and the filtrate concentrated to give a second crop. The combined crops were washed with diethyl ether and dried by oil pump vacuum to give *cis*-**8** as a white powder (0.1201 g, 0.1325 mmol, 77%), mp 125–128 °C. A similar reaction in toluene yielded comparable results. Calcd. for $C_{46}H_{96}P_2Pt$ (906.28): C 60.96; H 10.68. Found: C 59.77; H 10.51 [34].

NMR (CD_2Cl_2, δ/ppm): ^1H (500 MHz) 1.87–1.60 (m, 12H, CH_2), 1.45–1.21 (m, 72H, remaining CH_2), 0.29 (br s [33], 6H, J_{HPt} = 56.4 Hz [31], CH_3 *trans* to P), −0.28 (apparent br t [33], 6H, J_{HP} = 5.7 Hz, J_{HPt} = 43.9 Hz [31], CH_3 *trans* to CH_3); $^{13}C\{^1H\}$ (126 MHz) 31.5 (virtual t [15], J_{CP} = 5.1 Hz, $PCH_2CH_2CH_2$), 30.02 (s, CH_2), 29.96 (s, CH_2), 29.7 (s, CH_2), 29.3 (s, CH_2), 24.0 (s, PCH_2CH_2), 22.6 (m, PCH_2), 4.9 (dd, $J_{CP(cis)}$ = 8.4 Hz, $J_{CP(trans)}$ = 129 Hz, CH_3 *trans* to P), −13.2 (t, J_{CP} = 5.2 Hz, J_{CPt} = 407 Hz [31], CH_3 *trans* to CH_3); $^{31}P\{^1H\}$ (202 MHz) −43.4 (s, J_{PPt} = 1215 Hz) [31].

Crystallography. A. A solution of *trans*-**7** in diethyl ether was layered with ethanol. After 2 d, brown crystals were collected, and data obtained as outlined in Table s1. Cell parameters were obtained from 45 frames using a 1° scan and refined with 57,811 reflections. Integrated intensity information for each reflection was obtained by reduction of the data frames with the program APEX3 [35]. Lorentz and polarization corrections were applied. Data were scaled, and absorption corrections were applied using the program SADABS [36]. The space group was determined from systematic reflection conditions and statistical tests. The structure was solved using XT/XS in APEX3 [35,37]. The structure was refined (weighted least squares refinement on F^2) to convergence [37,38]. Olex2 was employed for the final data presentation. All non-hydrogen atoms were refined with anisotropic thermal parameters. Hydrogen atoms were placed in idealized positions and refined using a riding model. Appropriate restraints and/or constraints were applied to keep the bond distances, angles, and thermal ellipsoids meaningful. The absence of additional symmetry and voids were confirmed using PLATON (ADDSYM) [39].

B. A solution of *trans*-**8** in diethyl ether was allowed to slowly concentrate at 4 °C. After 2 d, colorless plates were collected. Data were obtained as outlined in Table s1 and treated as detailed for *trans*-**7** in A (cell parameters from 45 frames, 1° scan, refined with 86,542 reflections). For the $(CH_2)_{14}$ (but not $PtMe_4$) segments, elongated and unusual thermal ellipsoids suggested significant disorder. Given the data quality, no efforts were made to model the disorder. Rather, strong restraints were used to keep the thermal ellipsoids meaningful.

C. A saturated diethyl ether solution of *trans*-**5** was allowed to slowly concentrate at −35 °C. After 5 d, yellow blocks were collected, and data obtained as outlined in Table s1. Final cell parameters were obtained from 2404 frames using a 1° scan and refined with 54,027 reflections. Integrated intensity information for each reflection was obtained by reduction of the data frames with the program APEX4 [35]. Lorentz and polarization corrections were applied. Data were scaled, and absorption corrections were applied using the program SADABS [36]. The space group ($P4_3$ (#78)) was determined from systematic reflection conditions and statistical tests. The structure was solved using XT in APEX4 [35,37]. The structure was refined (weighted least squares refinement on F^2) to convergence [37,38]. Olex2 was employed for the final data presentation. Hydrogen atoms were placed in idealized positions and refined using a riding model. All non-hydrogen atoms were refined with anisotropic thermal parameters. Unusual elongated thermal ellipsoids suggested significant disorder of the $(CH_2)_{14}$ chains, which was successfully modeled by two positions (restraining bond distances and angles to idealized values; occupancy ratios 0.56:0.44 (chain 1), 0.57:0.43 (chain 2), and 0.69:0.31 (chain 3)). Strong restraints were used to keep the thermal ellipsoids meaningful. The absence of additional symmetry and voids were confirmed using PLATON [39]. The Flack parameter (0.20(3)) [40] suggested but did not fully confirm the absolute configuration of the chiral space group.

Supplementary materials

CCDC 2,262,793, 2,262,794, 2,262,795, and 2,262,796 contains the supplementary crystallographic data for *trans*-**5**, *trans*-**7** (two independent structure determinations) and *trans*-**8**. These can be obtained free of charge via http://www.ccdc.cam.ac.uk/conts/retrieving.html, or from the Cambridge Crystallographic Data centre, 12 Union Road, Cambridge CB2 1EZ, UK; fax: (+44) 1223–336–033; or e-mail: deposit@ccdc.cam.ac.uk. Additional supplementary data for this article can be found online at https://doi.org/10.1016/j.jorganchem.2023.xxxx (representative NMR spectra).

Declaration of Competing Interest

The authors declare that there are no financial interests/personal relationships that may be considered as potential competing interests:

John A. Gladysz reports financial support was provided by the US National Science Foundation.

Data availability

Data will be made available on request.

Acknowledgments

The authors thank the US National Science Foundation (NSF) for support (CHE-1566601, CHE-1900549), and Dr. Tobias Fiedler and Mr. Yi Shu for some preliminary observations.

Supplementary materials

Supplementary material associated with this article can be found, in the online version, at doi:10.1016/j.jorganchem.2023.122789.

References

[1] L.M. Rendina, T.W. Hambley, Platinum. In Comprehensive Coordination Chemistry II, J.A. McCleverty, T.J. Meyer, Editors-in-Chief. Elsevier, Amsterdam; Volume 6 (Fenton, D. E., volume Editor), pp. 673–745.

[2] Platinum complexes of the type **II** most relevant to this work (a) A.J. Nawara-Hultzsch, M. Stollenz, M. Barbasiewicz, S. Szafert, T. Lis, F. Hampel, N. Bhuvanesh, J.A. Gladysz, Gyroscope-Like Molecules Consisting of PdX_2/PtX_2 Rotators within Three-Spoke Dibridgehead Diphosphine Stators: Syntheses, Substitution Reactions, Structures, and Dynamic Properties, Chem. Eur. J. 20 (2014) 4617–4637, doi:10.1002/chem.201304419; (b) D. Taher, A.J. Nawara-Hultzsch, N. Bhuvanesh, F. Hampel, J.A. Gladysz, Mono- and disubstitution reactions of gyroscope like complexes derived from Cl-Pt-Cl rotators within cage like dibridgehead diphosphine ligands, J. Organomet. Chem. 821 (2016) 136–141, doi:10.1016/j.jorganchem.2016.03.022; (c) S. Kharel, H. Joshi, N. Bhuvanesh, J.A. Gladysz, Syntheses, Structures, and Thermal Properties of Gyroscope-like Complexes Consisting of $PtCl_2$ Rotators Encased in Macrocyclic Dibridgehead Diphosphines $P((CH_2)n)3P$ with Extended Methylene Chains (n = 20/22/30), and Isomers Thereof, Organometallics 37 (2018) 2991–3000, doi:10.1021/acs.organomet.8b00345; (d) Y. Zhu, A. Ehnbom, T. Fiedler, Y. Shu, N. Bhuvanesh, M.B. Hall, J.A. Gladysz, Platinum(II) alkyl complexes of chelating dibridgehead diphosphines $P((CH_2)n)3P$ (n = 14, 18, 22); facile *cis*/*trans* isomerizations interconverting gyroscope and parachute like adducts, Dalton Trans. 50 (2021) 12457–12477, doi:10.1039/D1DT02321G.

[3] Rhodium complexes of the type **II** (a) A.L. Estrada, T. Jia, N. Bhuvanesh, J. Blümel, J.A. Gladysz, Substitution and Catalytic Chemistry of Gyroscope-Like Complexes Derived from Cl-Rh-CO Rotators and Triply *trans* Spanning Di(trialkylphosphine) Ligands, Eur. J. Inorg. Chem. (2015) 5318–5321. 2015, doi:10.1002/ejic.201500953; (b) A.E. Estrada, L. Wang, N. Bhuvanesh, F. Hampel, J.A. Gladysz, Syntheses, Structures, Reactivities, and Dynamic Properties of Gyroscope Like Complexes Consisting of $Rh(CO)(X)$ or $Rh(CO)_2(I)$ Rotators and Cage-Like *trans* Aliphatic Dibridgehead Diphosphine Stators, Organometallics 41 (2022) 733–749, doi:10.1021/acs.organomet.1c00708.

[4] Iron complexes of the type **II** (a) G.M. Lang, T. Shima, L. Wang, K.J. Cluff, K. Skopek, F. Hampel, J. Blümel, J.A. Gladysz, Gyroscope-Like Complexes Based on Dibridgehead Diphosphine Cages That Are Accessed by Three-Fold Intramolecular Ring Closing Metatheses and Encase $Fe(CO)_3$, $Fe(CO)_2(NO)^+$, and $Fe(CO)_3(H)^+$ Rotators, J. Am. Chem. Soc. 138 (2016) 7649–7663, doi:10.1021/jacs.6b03178; (b) G.M. Lang, D. Skaper, F. Hampel, J.A. Gladysz, Synthesis, reactivity, structures, and dynamic properties of gyroscope like iron complexes with dibridgehead diphosphine cages: pre- vs. post-metathesis substitutions as routes to adducts with neutral dipolar Fe(CO)(NO)(X) rotors, Dalton Trans. 45 (2016) 16190–16204, doi:10.1039/C6DT03258C.

[5] Octahedral rhenium and osmium complexes of the type **II** (a) T. Fiedler, N. Bhuvanesh, F. Hampel, J.H. Reibenspies, J.A. Gladysz, Gyroscope like molecules consisting of trigonal or square planar osmium rotators within three-spoked dibridgehead diphosphine stators: syntheses, substitution reactions, structures, and dynamic properties, Dalton Trans. 45 (2016) 7131–7147, doi:10.1039/C6DT00692B; (b) G.D. Hess, T. Fiedler, F. Hampel, J.A. Gladysz, Octahedral Gyroscope-like Molecules Consisting of Rhenium Rotators Within Cage-like Dibridgehead Diphosphine Stators: Syntheses, Substitution Reactions, Structures, and Dynamic Properties, Inorg. Chem. 56 (2017) 7454–7469, doi:10.1021/acs.inorgchem.7b00909.

[6] (a) Y. Zhu, M. Stollenz, S.R. Zarcone, S. Kharel, H. Joshi, N. Bhuvanesh, J.H. Reibenspiess, J.A. Gladysz, Syntheses, homeomorphic and configurational isomerizations, and structures of macrocyclic aliphatic dibridgehead diphosphines: molecules that turn themselves inside out, Chem. Sci. 13 (2022) 13368–13386, doi:10.1039/D2SC04724A; (b) Improved synthetic route: S.R. Zarcone, N. Bhuvanesh, J.A. Gladysz, manuscript in preparation.

[7] A.L. Estrada, L. Wang, G. Hess, F. Hampel, J.A. Gladysz, Square Planar and Octahedral Gyroscope-Like Metal Complexes Consisting of Dipolar Rotators Encased in Dibridgehead Di(triaryl)phosphine Stators: Syntheses, Structures, Dynamic Properties, and Reactivity, Inorg. Chem. 61 (2022) 17012–17025, doi:10.1021/acs.inorgchem.2c02855.

[8] A. Ehnbom, J.A. Gladysz, Gyroscopes and the Chemical Literature, 2002-2020: Approaches to a Nascent Family of Molecular Devices, Chem. Rev. 121 (2021) 3701–3750, doi:10.1021/acs.chemrev.0c01001.

[9] Y. Zhu, T. Fiedler, J.A. Gladysz, A quest for platinum(0) adducts of the macrocyclic dibridgehead diphosphine $P((CH_2)_{14})_3P$, ChemRxiv (2023), doi:10.26434/chemrxiv-2023-r8jlg.

[10] S. Kharel, H. Joshi, S. Bierschenk, M. Stollenz, D. Taher, N. Bhuvanesh, J.A. Gladysz, Homeomorphic isomerization as a design element in container molecules; binding, displacement, and selective transport of MCl_2 species (M = Pt, Pd, Ni), J. Am. Chem. Soc. 139 (2017) 2172–2175, doi:10.1021/jacs.6b12788.

[11] H. Joshi, S. Kharel, A. Ehnbom, K. Skopek, G.D. Hess, T. Fiedler, F. Hampel, N. Bhuvanesh, J.A. Gladysz, Three-fold intramolecular ring closing alkene metatheses of square planar complexes with *cis* phosphorus donor ligands $P(X(CH_2)_mCH{=}CH_2)_3$ (X = –, m = 5-10; X = O, m = 3-5): syntheses, structures, and thermal properties of macrocyclic dibridgehead diphosphorus complexes, J. Am. Chem. Soc. 140 (2018) 8463–8478, doi:10.1021/jacs.8b02846.

[12] R.K. Tanaka, Rhodium Catalysis in Organic Synthesis: Methods, Wiley-VCH, Weinheim, Germany, 2019.

[13] (a) M. Lersch, M. Tilset, Mechanistic Aspects of C-H Activation by Pt Complexes, Chem. Rev. 105 (2005) 2471–2526, doi:10.1021/cr030710y; (b) J.J. Topczewski, M.S. Sanford, Carbon-hydrogen (C-H) bond activation at Pd^{IV}: a Frontier in C-H functionalization catalysis, Chem. Sci. 6 (2015) 70–76, doi:10.1039/C4SC02591A.

[14] (a) F.J. Strauss, D. Cantillo, J. Guerra, C.O. Kappe, A laboratory-scale continuous flow chlorine generator for organic synthesis, React. Chem. Eng. 1 (2016) 472–476, doi:10.1039/C6RE00135A; (b) X.F. Zhao, C. Zhang, Iodobenzene Dichloride as a Stoichiometric Oxidant for the Conversion of Alcohols into Carbonyl Compounds; Two Facile Methods for its Preparation, Synthesis 4 (2007) 551–557, doi:10.1055/s-2007-965889.

[15] W.H. Hersh, False AA'X Spin-Spin Coupling Systems in ^{13}C NMR: Examples Involving Phosphorus and a 20-year-old Mystery in Off-Resonance Decoupling, 1997. The J values in this paper represent the distance between adjacent peaks in the apparent triplet. J. Chem. Educ, 74 1485–1488, doi:10.1021/ed074p1485.

[16] (a) A. Pidcock, R.E. Richards, L.M. Venanzi, ^{195}Pt-^{31}P nuclear spin coupling constants and the nature of the *trans*-effect in platinum complexes, J. Chem. Soc. A (1966) 1707–1710, doi:10.1039/J19660001707; (b) P.L. Goggin, R.J. Goodfellow, S.R. Haddock, J.R. Knight, F.J.S. Reed, B.F. Taylor, Vibrational spectra and nuclear magnetic resonance parameters of some platinum(IV) complexes $[PtX_4L_2]$ and $[PtX_5L]^-$ (X = Cl, Br, or I; L = NMe_3, PMe_3, $AsMe_3$, or SMe_2), J. Chem. Soc. Dalton. Trans. (1974) 523–533, doi:10.1039/DT9740000523.

[17] M. Lashanizadehgan, M. Rashidi, J.E. Hux, R.J. Puddephatt, S.S.M. Ling, The synthesis, characterization and reactions of a binuclear tetramethylplatinum(IV) complex, J. Organomet. Chem. 3 (1984) 317–322, doi:10.1016/0022-328X(84)80318-6.

[18] M.D. Levin, D.M. Kaphan, C.M. Hong, R.G. Bergman, K.N. Raymond, F.D. Toste, Scope and mechanism of cooperativity at the intersection of organometallic and supramolecular catalysis, J. Am. Chem. Soc. 138 (2016) 9682–9693 see pages s6 and s8 of their supporting information, doi:10.1021/jacs.6b05442.

[19] (a) For J_{PPt} values of additional complexes of the formula *cis*-$Pt(Me)_4$(diphosphine) (1119-1148 Hz), see D.M. Crumpton-Bregel, K.I. Goldberg, Mechanisms of C-C and C-H Alkane Reductive Eliminations from Octahedral Pt(IV): Reaction via Five-Coordinate Intermediates or Direct Elimination? J. Am. Chem. Soc. 125 (2003) 9442–9456, doi:10.1021/ja029140u; (b) H.R. Shahsavari, M. Rashidi, S.M. Nabavizadeh, S. Habibizadeh, F.W. Heinemann, A Tetramethylplatinum(IV) Complex with 1,1′Bis(diphenylphosphanyl)ferrocene Ligands: Reaction with Trifluoroacetic acid, Eur. J. Inorg. Chem. (2009) 3814–3820, doi:10.1002/ejic.200900454.

[20] V.Y. Kukushkin, V.K. Belsky, V.E. Konovalov, E.A. Aleksandrova, E.Y. Pankova, A.I. Moiseev, Deoxygenation of coordinated sulfoxides and oxidation of the metal ion in the Pt(II) complexes using HX (X = Cl, Br): a convenient proce-

dure for the preparation of thioether compounds of Pt(IV). X-ray structure of potassium trichloro(diethyl sulfoxide)platinate(II), Phosphorus, Sulfur and Silicon 69 (1992) 103–117, doi:10.1080/10426509208036859.

[21] The isolation of *trans*-**8** has prompted spirited discussions among reviewers of this manuscript and the corresponding doctoral dissertation. One individual suggested that a species functionally equivalent to $CH_3OOMgBr$, formed by oxidation of the Grignard reagent, is the key to accessing the platinum(IV) manifold. In our opinion, the close agreement of the widely diverging J_{PPt} values of *cis*- and *trans*-**8** with those of *cis*- and *trans*-$Pt(Me)_4(PMe_3)_2$ (see text) strongly argues against any artifact associated with the crystal structure.

[22] T.A. Perera, M. Masjedi, P.R. Sharp, Photoreduction of Pt(IV) chloro complexes: substrate chlorination by a triplet excited state, Inorg. Chem. 53 (2014) 7608–7621, doi:10.1021/ic5009413.

[23] A.R. Karikachery, H.B. Lee, M. Masjedi, A. Ross, M.A. Moody, X. Cai, M. Chui, C.D. Hoff, P.R. Sharp, High quantum yield bromine photoelimination from mononuclear platinum(IV) complexes, Inorg. Chem. 52 (2013) 4113–4119, doi:10.1021/ic4004998.

[24] (a) L. Aslanov, R. Mason, A.G. Wheeler, P.O. Whimp, Stereochemistries of and Bonding in Complexes of Third-row Transition-metal Halides with Tertiary Phosphines, Chem. Commun. (1970) 30–31, doi:10.1039/C29700000030; (b) Crystallographic comparisons outside of the bond lengths quoted are not possible, as this structure is missing from the CCD, as confirmed by a private communication.

[25] A. Bondi, Van der waals volumes and radii, J. Phys. Chem. 68 (1964) 441–451, doi:10.1021/j100785a001.

[26] The relative σ donor and π acceptor properties of a variety of ligands are treated in this review B.J. Coe, S.J. Glenwright, Trans-effects in octahedral transition metal complexes, Coord. Chem. Rev 203 (2000) 5–80, doi:10.1016/S0010-8545(99)00184-8.

[27] T.G. Appleton, H.C. Clark, L.E. Manzer, The *trans*-influence: its measurement and significance, Coord. Chem. Rev. 10 (1973) 335–422, doi:10.1016/S0010-8545(00)80238-6.

[28] (a) M.P. Mitoraj, H. Zhu, A. Michalak, T. Ziegler, On the Origin of the Trans-Influence in Square Planar d^8-Complexes: A Theoretical Study, Int. J. Quantum Chem. 109 (2009) 3379–3386, doi:10.1002/qua.21910; (b) B. Pinter, V. Van Speybroeck, M. Waroquier, P. Geerlings, F. De Proft, Trans effect and *trans* influence: importance of metal mediated ligand-ligand repulsion, Phys. Chem. Chem. Phys. 15 (2013) 17354–17365, doi:10.1039/C3CP52383G; (c) A.C. Tsipis, *Trans*-Philicity (*trans*-Influence/*trans*-Effect) Ladders for Square Planar Platinum(II) Complexes Constructed by ^{35}Cl NMR Probe, J. Comput. Chem. 40 (2019) 2550–2562, doi:10.1002/jcc.26031.

[29] R.D. Baechler, K. Mislow, The effect of structure on the rate of pyramidal inversion of acyclic phosphines, J. Am. Chem. Soc 92 (1970) 3090–3093, doi:10.1021/ja00713a028.

[30] M.E. Howe, M.A. Garcia-Garibay, The roles of intrinsic barriers and crystal fluidity in determining the dynamics of crystalline molecular rotors and molecular machines, J. Org. Chem. 84 (2019) 9835–9849 and earlier references therein, doi:10.1021/acs.joc.9b00993.

[31] This coupling represents a satellite (d, ^{195}Pt = 33.8%) and is not reflected in the peak multiplicity given.

[32] Due to the poor signal/noise, *J* values for this peak cannot be confidently assigned.

[33] These couplings are clearly non-first-order, as depicted in the SI. Similar patterns have been reported for other complexes of the formula *cis*-$Pt(Me)_4$(diphosphine) [18,19]. For simulations and fully delineated spin systems in related complexes, see B.K. Collins, N. Weisbach, F. Hampel, N. Bhuvanesh, J.A. Gladysz, Building blocks for molecular polygons based upon platinum vertices and polyynediyl edges, Organometallics 42 (2023), in press, doi:10.1021/acs.organomet.2c0057.

[34] This microanalysis poorly agrees with the empirical formula, but is nonetheless reported as the best obtained to date. The NMR spectra indicate high purities.

[35] APEX3Program For Data Collection On Area Detectors, BRUKER AXS Inc., Madison, WI, USA, 2012.

[36] G.M. Sheldrick, SADABS, BRUKER AXS Inc., Madison, WI, USA, 2001.

[37] (a) G.M. Sheldrick, A short history of *SHELX*, Acta Crystallogr., Sect. A 64 (2008) 112–122, doi:10.1107/S0108767307043930; (b) G.M. Sheldrick, *SHELXT* – Integrated space-group and crystal-structure determination, Acta Crystallogr., Sect. A. 71 (2015) 3–8, doi:10.1107/S2053273314026370.

[38] O.V. Dolomanov, L.J. Bourhis, R.J. Gildea, J.A.K. Howard, H. Puschmann, *OLEX2*: a complete structure solution, refinement and analysis program, J. Appl. Crystallogr. 42 (2009) 339–341, doi:10.1107/S0021889808042726.

[39] A.L. Spek, Single-crystal structure validation with the program *PLATON*, J. Appl. Crystallogr. 36 (2003) 7–13, doi:10.1107/S0021889802022112.

[40] H.D. Flack, On enantiomorph-polarity estimation, Acta Cryst. A39 (1983) 876–881 (theory for correct and inverted configurations: 0 and 1), doi:10.1107/S0108767383001762.